Heterobimetallic copper–barium complexes for deposition of composite oxide thin films†

Asif Ali Tahir,[a] Muhammad Mazhar,*[a] Mazhar Hamid,[a] Matthias Zeller[b] and Allen D. Hunter[b]

Received (in Gainesville, FL, USA) 24th December 2008, Accepted 16th March 2009
First published as an Advance Article on the web 2nd April 2009
DOI: 10.1039/b823024b

Heterobimetallic molecular precursors $[Ba(dmap)_4Cu_4(OAc)_6{\cdot}THF]$ (**1**) and $[Ba(dmap)_4Cu_4(TFA)_6{\cdot}THF]$ (**2**) [dmap = *N*,*N*-dimethylaminopropanolate, OAc = acetate and TFA = trifluoroacetate] for the deposition of barium–copper composite oxide thin films, were prepared by the interaction of $Ba(dmap)_2$ with $Cu(OAc)_2$ for **1** and $Cu(TFA)_2$ for **2**, in THF. Both heterobimetallic complexes were characterized by melting point, elemental analysis, FT-IR spectroscopy, mass spectrometry and single crystal X-ray diffraction. X-Ray crystallography shows that complex **1** crystallizes in the orthorhombic space group $P2_12_12_1$ with the cell dimensions a = 11.2621(11) Å, b = 18.2768(17) Å and c = 24.541(2) Å, while complex **2** crystallizes in the monoclinic space group $C2/c$ with a = 23.9288(14) Å, b = 19.8564(12) Å, c = 25.5925(15) Å and β = 112.4390(10)°. Thermal gravimetric analysis shows that both complexes **1** and **2** undergo controlled thermal decomposition at 450 °C and 400 °C, respectively, to give mixed metal oxide composite thin films. Scanning electron microscopy (SEM), energy dispersive X-ray (EDX) and X-ray powder diffraction (XRD) analyses of the thin films suggest the formation of good quality crystalline thin films of $BaCuO_2$–CuO composites from both **1** and **2**, with average grain sizes of 105 to 175 nm and 110 to 205 nm, respectively.

Introduction

The discovery of high T_c $YBa_2Cu_3O_x$ and other ceramic superconductors[1,2] has intensified research into the development of new copper and barium precursors for solution route processing towards these materials.[3] The commonly used chemical method for the production of thin films of superconductor materials is *via* either chemical vapor deposition (CVD) or *via* sol–gel processes.[4] The CVD method has been shown to be able to produce good quality films, but it is often limited by the unavailability of precursor compounds with sufficient volatility.[5] In an alternative approach the corresponding precursor compounds that contain all the desired components are mixed together in solution and are then coated onto the substrate *via* spin coating or a dip coating process. Another promising technique for the deposition of thin films of ceramic materials is ultrasonic aerosol assisted chemical vapour deposition (AACVD) which provides the possibility of better control of the deposition conditions. The most important requirements of all the solution techniques are that all components should be highly soluble in the solvent of choice, *e.g.* a standard organic solvent. One way to improve the solubility of the metal compounds in such organic solvents is to bind suitable organic ligands to the metal centers. Due to the inherent different nature of the metal ions present in superconductors, ligands have to be chosen based on their suitability for each metal. For example, a copper(II) ion will bind well with oxygen or nitrogen donor atoms in an essentially covalent fashion while barium(II) and yttrium(III) ions have a poor affinity towards neutral nitrogen donor atoms, but, due to their ionic nature, a relatively good affinity towards negatively charged donor atoms such as oxides or alkoxides.[6]

Keeping these requirements for the synthesis of materials by AACVD of mixed metal ceramic materials in mind, we have focused our research on two areas: the design and synthesis of discrete molecular precursors for ceramic superconductors and their subsequent use for the deposition of thin films by aerosol assisted chemical vapour deposition. Following our previous work directed towards the design of heterobimetallic complexes for mixed metal oxide systems,[7,8] our strategy was therefore to employ bifunctional ligands which contain both a neutral and a negatively charged coordinating site so that they are able to bind to two different types of metal ions. An example of such a ligand is the bifunctional amino alcohol ligand *N*,*N*-dimethylamino-1-propanol (dmapH). In our previous investigation we found that it can coordinate in a variety of coordination modes and did often allow for the formation of highly soluble molecular precursors.[9,10] Application of this ligand to the copper–barium system yielded two promising mixed metal precursors, which were both obtained in yields around 90% under mild reaction conditions at room temperature. Reaction of $Ba(dmap)_2$

[a] *Department of Chemistry, Quaid-I-Azam University, Islamabad 45320, Pakistan. E-mail: mazhar42pk@yahoo.com; Fax: +92(0)5190642241; Tel: +92(0)5190642106*
[b] *STaRBURSTT-Cyberdiffraction Consortium @ YSU & Department of Chemistry, Youngstown State University, 1 University Plaza, Youngstown, OH 44555-3663, USA*

† CCDC reference numbers 724118 and 724119. For crystallographic data in CIF or other electronic format see DOI: 10.1039/b823024b

with $Cu(OOCCH_3)_2$ and $Cu(OOCCF_3)_2$ gave crystalline $[Ba(dmap)_4Cu_4(OAc)_6 \cdot THF]$ (**1**) and $[Ba(dmap)_4Cu_4(TFA)_6 \cdot THF]$ (**2**) [dmapH = *N*,*N*-dimethylaminopropanol and OAc = acetate and TFA = trifluoroacetate]. Both complexes **1** and **2** are soluble in THF and toluene under the experimental conditions of AACVD and both deposit homogeneous good quality thin films of barium copper oxides that may find possible uses in industrial and other technological applications.

Experimental section

All manipulations were carried out under an inert atmosphere of dry nitrogen using Schlenk tube and glovebox techniques. Solvents were rigorously dried and distilled using standard methods. Barium metal, $Cu(OAc)_2$, lithium metal, trifluoroacetic acid, *N*,*N*-dimethylamino-1-propanol and all other reagents were purchased from Aldrich Chemicals. Melting points were recorded on a Mitamura Riken Kogyo (MT-D) apparatus and are uncorrected. Elemental analyses were performed using a CHN Analyzer LECO model CHNS-932. FAB mass spectra were recorded using a JMS-HX-1100 mass spectrometer of Jeol, Japan. FT-IR spectra were recorded with a Bio-Red Excalibur FT-IR model FTs 300MX spectrometer from KBr discs.

Controlled thermal analyses of the complexes were carried out using a Perkin Elmer thermogravimetric analyzer TGA7 with a computer interface. The measurements were carried out in alumina crucibles under an atmosphere of flowing nitrogen gas (25 ml min^{-1}) at a heating rate of 10 °C min^{-1}.

Single crystal diffraction data of complexes **1** and **2** were collected on a Bruker AXS SMART APEX CCD diffractometer at 100(2) K using monochromatic MoKα radiation with an Ω scan technique. The unit cells were determined using SMART[11] and SAINT+[12] and the data were corrected for absorption using SADABS in SAINT+. The structures were solved by direct methods and refined by full matrix least squares against F^2 with all reflections using SHELXTL.[13] Refinement of extinction coefficients was found to be insignificant. All non-hydrogen atoms were refined anisotropically.

In the structure of **1** a solvate THF molecule is disordered around a general site with an occupancy ratio of 0.75(2) to 0.25(2). The two moieties were restrained to have the same geometries within a standard deviation of 0.02, the atoms were restrained to be isotropic within a standard deviation of 0.1, and the atoms within a ring were restrained to have similar anisotropic components within a standard deviation of 0.03 (SIMU and DELU restraints in SHELXTL).

In **2** a THF molecule is disordered around a two fold axis over two sites, one located directly on the two fold axis, the other around it. The occupancy ratio of the two sites is 0.44(1) to 0.46(1). The C–C bond distances in the disordered molecules were restrained to be 1.543 Å, the O–C distances to be 1.426 Å. Three of the CF_3 groups are disordered each over two positions with occupancy ratios of 0.60(1) to 0.40(1), 0.43(2) to 0.57(2) and 0.48(1) to 0.52(1). The C–F and F–F distances were restrained to be each the same for the disordered moieties within a standard deviation of 0.02, and the disordered fluorine atoms were restrained to be isotropic within a standard deviation of 0.1. The highest peak for compound **2** has a value of 2.85 electrons per cubic Å and is located 0.03 Å from the barium atom.

The phase and crystallinity of deposited films were characterized using a Bruker AXS D8 Advance X-ray diffractometer with primary monochromatic high-intensity CuKα (λ = 0.154184 nm) radiation using a PSD detector. A range of 2θ (from 10.00 to 75.00) was scanned, to cover the diffraction patterns of the oxide phase. The percentage compositions of both the phases were determined using the "PANanalytical X'Pert PRO" XRD software which calculates the percentage composition of each phase based on the 2θ value and intensity of the standard ICDD pattern and the residual XRD pattern. Surface morphology of thin films was studied by using a field emission gun scanning electron microscope (Leo 1530 VP) at an accelerating voltage of 5 kV, and a working distance of 6 mm.

Synthesis of $Ba(dmap)_4Cu_4(OAc)_6 \cdot THF$

Barium metal (0.50 g, 3.64 mmol) was added to a stirred solution of dmapH (1.5 g, 14.59 mmol) in 25 ml of dry toluene. The mixture was stirred for 2 h until all pieces of barium were consumed. $Cu(OAc)_2$ (2.90 g, 14.59 mmol) was then added with stirring to the above solution of $Ba(dmap)_2$ and the mixture was stirred for 12 h to obtain a deep blue solution, which was filtered through a cannula to remove any traces of solid residue. The reaction mixture was evaporated to dryness under vacuum, and the solid was redissolved in 10 ml of THF and placed in a refrigerator at −10 °C for crystallization. Blue coloured crystals were obtained after 3 days in 85% yield based on barium metal used. Mp: 110 °C; analysis: calc. for $C_{36}H_{74}BaCu_4N_4O_{17}$ C, 35.22; H, 6.03; N, 4.56; found C, 35.75; H, 6.45; N, 4.70%. FT-IR/cm^{-1}: 2977w, 2927w, 2363w, 2344w, 1582s, 1405s, 1336s, 1193w, 1089m, 1021w, 947m, 869m, 839s, 677m, 619m, 537w, 376w. FAB+ *m*/*z*: 1156 $[M - THF]^+$, 1034 $[M - 2OAc]^+$, 955 $[M - 2dmap]^+$, 896 $[M - (dmap)_2(OAc)]^+$, 613 $[M/2]^+$, 512 $[M/2 - dmap]^+$, 389 $[M/2 - (OAc)_2(dmap)]^+$, 287 $[M/2 - (OAc)_2(dmap)_2]^+$, 100 $[dmap - H]^+$, 58 $[OAc - H]^+$; TGA: 20–165 °C (11.85% wt. loss); 165–289 °C (45.96% wt. loss); 289–412 °C (residue 31.10%).

Synthesis of $Ba(dmap)_4Cu_4(TFA)_6 \cdot THF$

Barium metal (0.50 g, 3.64 mmol) was added to a stirred solution of dmapH (1.5 g, 14.59 mmol) in dry THF (10 ml). The mixture was stirred for 2 h until all pieces of barium were consumed. $Cu(TFA)_2$ (2.90 g, 14.59 mmol) was prepared by the reaction of 1.83 g (14.59 mmol) of $Cu(OMe)_2$ with 1.66 g (14.59 mmol) of trifluoroacetic acid in 15 ml THF. The THF solution of $Cu(TFA)_2$ was added dropwise to the stirring solution of $Ba(dmap)_2$ and after 5 h the deep blue solution was filtered through a cannula to remove any traces of solid residue. The reaction mixture was evaporated to dryness under vacuum, and the solid was redissolved in 5 ml of THF and light blue coloured crystals were obtained after 3 days with 95% yield based on barium metal used. Mp: 195 °C; analysis: calc. for $C_{36}H_{56}N_4F_{18}BaCu_4O_{17}$ C, 26.94; H, 3.43; N, 3.69;

found C, 27.04; H, 3.66; N, 3.68%. FT-IR/cm^{-1}: 2918w, 2872w, 2749w, 2539w, 1660s, 1449s, 1385w, 1199s, 1137m, 1039m, 1045s, 107s, 942m, 834s, 800s, 726m, 619m, 570w, 521w. FAB+ *m*/*z*: 1484 [M − THF]$^+$, 1452 [M − dmap]$^+$, 1412 [M − dmap]$^+$, 1343 [M − (dmap)(THF)]$^+$, 1307 [M − (dmap)$_2$]$^+$, 1244 [M − Cu(dmap)$_2$]$^+$, 1000 [M/2 + 2TFA]+, 975 [M/2 + 2dmap]$^+$, 922 [M − BaCu$_2$(TFA)$_2$(dmap)]$^+$, 896 [M/2 + Ba]$^+$, 843 [M/2 + $C_5H_{12}N$]$^+$, 801 [M/2 + OC_2H_4]$^+$, 772 [M/2 + O]$^+$, 723 [Cu$_2$(dmap)$_2$(TFA)$_2$]$^+$, 699 [Ba(TFA)$_5$]$^+$, 687 [Ba(dmap)$_3$(TFA)$_2$]$^+$, 619 [BaCu(dmap)$_3$-(TFA)]$^+$, 557 [Ba(dmap)$_3$(TFA)]$^+$, 508 [BaCu(dmap)$_3$]$^+$, 443 [Ba(dmap)$_3$]$^+$, 342 [Cu(dmap)(TFA)]$^+$, 239 [Ba(dmap)$_3$]$^+$, 207 [CuO$_2$(TFA)]$^+$, 166 [Cu(dmap)]$^+$, 136 [Ba]$^+$, 102 [dmap]$^+$; TGA: 195–223 °C (9.06% wt. loss); 223–269 °C (32.5% wt. loss); 269–400 °C (residue 29.74%).

Deposition of thin films by AACVD

Thin films from complexes **1** and **2** were deposited on commercially available soda glass slides by using a self designed ultrasonic aerosol assisted chemical vapor deposition assembly.[14] The glass substrate was cleaned prior to use by ultrasonically washing with distilled water, acetone and finally with ethyl alcohol. In a typical deposition, 25 ml of a 0.02 M solution in toluene of **1** and in THF of **2** were added to a round-bottomed flask. Air at a flow rate of 150 ml min^{-1} was used as the carrier gas, and the flow rate was controlled by an L1X linear flow meter. Substrate slides (2 cm × 2 cm) were placed inside the reactor tube and then heated up to 450 °C for **1** and 400 °C for **2**. The aerosols of the precursor solution were formed by keeping the round-bottomed flask in a water bath above the piezoelectric modulator of an ultrasonic humidifier. The generated aerosol droplets of the precursor were transferred into the hot wall zone of the reactor by the carrier gas. The reactor was placed in a tube furnace. In the case of complex **2** the carrier gas was passed through water before the aerosol flask to avoid the formation of barium fluoride. Alternatively, the addition of 2 ml of water in the precursor solution was also effective but some precipitates were left behind at the end of the deposition which decreased the barium content in the deposited films.

Result and discussion

Lewis acid–base adduct formation to produce heterobimetallic coordination complexes in good yield under mild conditions is a very promising method to design molecules for the deposition of thin films of a desired material.[15] This type of synthetic strategy aims to coordinatively saturate each metal center by the use of chelating ligands *e.g.* a carboxylate, a functionalized alcohol *etc.*, which enhance their stability, solubility, volatility and their shelf life. We have recently reported that the amino alcohol *N*,*N*-dimethylaminoethanol (dmaeH) can, as a ligand, bring two very different metal centers such as copper(II) and lanthanide metals together through binding *via* both the amino and the alkoxo site.[16,17] Since alkaline-earth metal ions behave quite similarly to the lanthanides due to their highly electropositive nature, the ligand bis(dimethylamino)-1-propanol (bdmap) was anticipated to be also a useful ligand for the synthesis of mixed-metal complexes involving alkaline-earth metals and the copper(II) ion. Indeed, several such mixed-metal complexes have been obtained readily by using the bdmap ligand.[18]

Two heterobimetallic Cu–Ba complexes were readily synthesized by simple synthetic procedures involving the mixing of the reactants in the proper molar ratios. Thus complexes Ba(dmap)$_4$Cu$_4$(OAc)$_6$·THF (**1**) and Ba(dmap)$_4$Cu$_4$(TFA)$_6$·THF (**2**) were prepared by reacting appropriate amounts of tetrameric *N*,*N*-dimethylaminopropanolato Ba(II) with 2 equivalents of Cu(OAc)$_2$ and Cu(TFA)$_2$ in THF at room temperature. The complexes are soluble in common organic solvents such as THF, toluene and alcohols and are stable in air under ambient conditions.

Both complexes **1** and **2** were characterized by their melting point, elemental analysis, FT-IR, TGA and single crystal X-ray diffraction. The FT-IR spectra display absorption bands characteristic of the carboxylate ligands that appear at 1582 and 1660 cm^{-1} for the asymmetric $\nu_{as}(CO_2)$ vibration and at 1405–1449 cm^{-1} due to the symmetric vibration for **1** and **2**, respectively. The difference of the values $\Delta = \nu_{as}(CO_2) - \nu_s(CO_2)$ is greater than 150 cm^{-1} suggesting that the carboxylate ligands are bridging between two metal centers.[19] In the case of complex **2**, very intense sharp absorption bands at 1199 and 1137 cm^{-1} correspond to the C–F vibrations[20] which are not observed in the case of complex **1**. Additional sharp bands due to the coordinated Lewis base are present which are shifted to lower frequencies with respect to those of the free ligand. The FAB mass spectra of both complexes **1** and **2** show the molecular ion peaks after the removal of the solvent molecules. The mass spectra of both the complexes show a well defined peak pattern, which reveals the stability of the complexes under experimental conditions.

Molecular structures of complexes 1 and 2

The molecular structures of complexes **1** and **2** are shown in Fig. 1 and Fig. 2, respectively. Selected material data, bond distances and angles are listed in Table 1 and Table 2. The

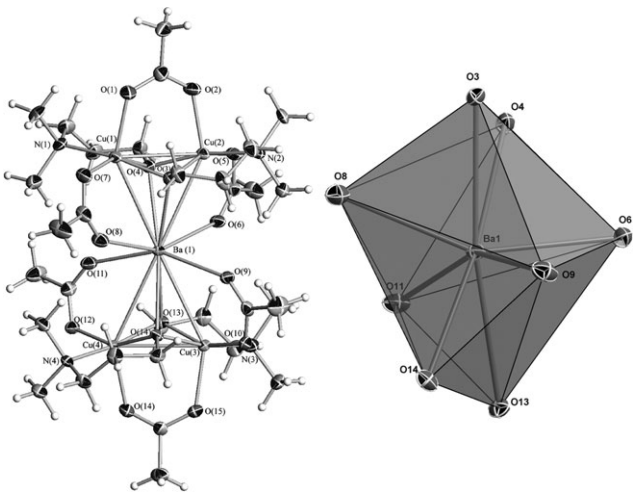

Fig. 1 Molecular structure of Ba(dmap)$_4$Cu$_4$(OAc)$_6$ and coordination sphere of Ba(1) in **1**. Ellipsoids are drawn at the 30% probability level. The solvent (THF) molecule is not shown for clarity.

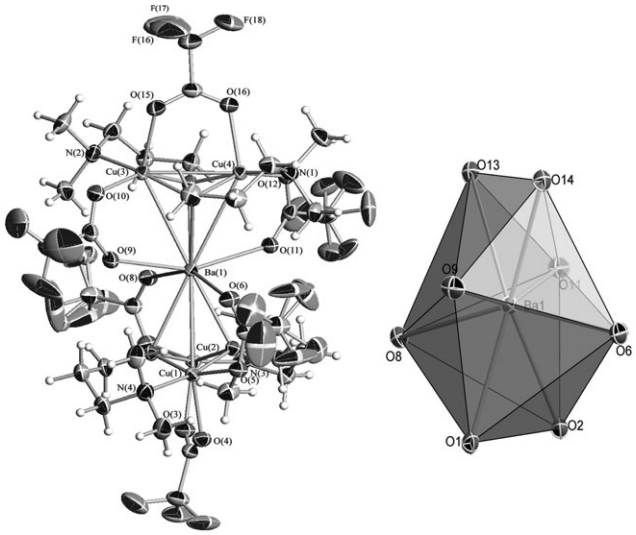

Fig. 2 Molecular structure of $Ba(dmap)_4Cu_4(TFA)_6$ and coordination sphere of Ba(1) in **2**. Ellipsoids are drawn at the 50% probability level. Three of the six CF_3 groups are disordered each over two positions. The solvent (THF) molecule is not shown for clarity.

molecules in both complexes are closely related and consist of two dicopper units with the formulas $[Cu_2(\mu\text{-dmap})_2(\mu\text{-OAc})_2]$ in complex **1** and $[Cu_2(\mu\text{-dmap})_2(\mu\text{-TFA})_2]$ in complex **2**. The barium ions are sandwiched between these two dicopper units. In the dicopper unit, the two copper(II) ions are bridged by two oxygen atoms from the two dmap ligands with normal Cu–O bond distances (1.96(2) Å), and are comparable with the known Cu–O bonds involving the dmap ligand.[21,22] The Cu–Cu separations in the dicopper units, Cul–Cu2 = 2.93(11) Å, and Cu3–Cu4 = 2.921 (7) Å, are comparable to those of previously reported dinuclear copper complexes.[23] The geometry around the copper centers in each dicopper unit is distorted square pyramidal and the CuO_4N core is made up from two bridging oxygen atoms of an acetate or TFA ligand (in **1** and **2**, respectively), from two triply bridged oxygen atoms of the dmap ligands and the remaining site is occupied by a coordinating nitrogen atom of the dmap ligand. The Cu–N bond lengths in both complexes **1** and **2** are in the range of 2.02(3)–2.07(6) Å which is slightly shorter than reported for similar complexes.[24]

The barium atom which is sandwiched between the two dicopper units has a coordination number of eight with a distorted square antiprismatic geometry. The coordination environment around the barium atom is made up by four bridging OAc/TFA ligands and four triply bridging oxygen atoms of the dmap ligands. The $Ba–O_{acetate}$ bond distances range from 2.69(5)–2.73(2) Å which are slightly shorter than the $Ba–O_{dmap}$ bond distances that range from 2.77(2)–2.91(2) Å.

Barium–oxygen bond distances in reported compounds span a considerable range, 2.60–3.00 Å.[25,26] For example, in the unit cell of the Y-123 superconductors ($YBa_2Cu_3O_{7-x}$), each BaO_4 layer is sandwiched by a Cu_4O_2 layer and a Cu_4O_4 layer.[27] The Ba–O distances between the Ba atom and the oxygen atoms in the Cu_4O_4 and Cu_4O_2 layers are much longer, 2.915 Å, than the Ba–O distances in the BaO_4 layer (2.750(3) Å). By sharing of the oxygen atom from the bdmap ligand between two copper and one barium centers and having

Table 1 Crystal data and structure refinement for compounds **1** and **2**

Empirical formula	$C_{36}H_{74}BaCu_4N_4O_{17}$	$C_{68}H_{104}Ba_2Cu_8F_{36}N_8O_{33}$
Moiety formula	$C_{32}H_{66}BaCu_4N_4O_{16}$, C_4H_8O	$2[C_{32}H_{66}BaCu_4F_{18}N_4O_{16}]$, C_4H_8O
Formula weight	1226.49	3028.66
Solvent	THF	THF
Cryst. habit, color	Block, blue	Block, blue
Temperature	100(2) K	100(2) K
Crystal system	Orthorhombic	Monoclinic
Space group	$P2_12_12_1$	$C2/c$
Unit cell dimensions	a = 11.2621(11) Å	a = 23.9288(14) Å
	b = 18.2768(17) Å	b = 19.8564(12) Å
	c = 24.541(2) Å	c = 25.5925(15) Å
		β = 112.4390(10)°
Volume/Å^3	5051.3(8)	11239.3(12)
Z	4	4
Density (calculated)/Mg m^{-3}	1.613	1.790
Absorption coefficient/mm^{-1}	2.491	2.302
F(000)	2504	6000
Crystal size	0.55 × 0.50 × 0.42 mm^3	0.40 × 0.35 × 0.30 mm^3
θ range for data collection	1.39 to 28.28°	1.38 to 28.28°
Index ranges	$-15 \le h \le 15$,	$-31 \le h \le 31$,
	$-22 \le k \le 24$,	$-26 \le k \le 26$,
	$-23 \le l \le 32$	$-28 \le l \le 34$
Reflections collected	34659	50829
Independent reflections	12431	13878
Absorption correction	Multi-scan	Multi-scan
Max. and min. transmission	0.351 and 0.228	0.501 and 0.447
Data/restraints/parameters	12431/150/619	13878/255/791
Goodness-of-fit on F^2	1.119	1.079
Final R indices [$I > 2\sigma(I)$]	$R1$ = 0.0629, w$R2$ = 0.1668	$R1$ = 0.0374, w$R2$ = 0.0961
R indices (all data)	$R1$ = 0.0680, w$R2$ = 0.1709	$R1$ = 0.0463, w$R2$ = 0.1069
Largest diff. peak and hole	9.961 and −1.407 e Å^{-3}	2.847 and −0.863 e Å^{-3}

Table 2 Selected bond distances and angles for complexes **1** and **2**

Bond distances/Å for **1**		Bond distances/Å for **2**		Bond angles/° for **1**		Bond angles/° for **2**	
Ba(1)–O(9)	2.692(5)	Ba(1)–O(8)	2.693(2)	O(9)–Ba(1)–O(11)	152.26(14)	O(9)–Ba(1)–O(8)	90.37(7)
Ba(1)–O(11)	2.697(5)	Ba(1)–O(9)	2.714(2)	O(9)–Ba(1)–O(8)	106.84(17)	O(9)–Ba(1)–O(6)	90.63(8)
Ba(1)–O(8)	2.707(5)	Ba(1)–O(6)	2.720(2)	O(9)–Ba(1)–O(6)	79.62(15)	O(9)–Ba(1)–O(11)	156.82(7)
Ba(1)–O(6)	2.718(5)	Ba(1)–O(11)	2.731(2)	O(9)–Ba(1)–O(14)	65.43(13)	O(9)–Ba(1)–O(14)	69.57(7)
Ba(1)–O(14)	2.834(4)	Ba(1)–O(14)	2.779(2)	O(9)–Ba(1)–O(4)	121.18(14)	O(9)–Ba(1)–O(2)	123.36(6)
Ba(1)–O(4)	2.837(5)	Ba(1)–O(2)	2.803(2)	O(9)–Ba(1)–O(3)	84.64(14)	O(9)–Ba(1)–O(13)	89.78(6)
Ba(1)–O(3)	2.851(4)	Ba(1)–O(13)	2.848(2)	O(9)–Ba(1)–O(13)	88.91(13)	O(9)–Ba(1)–O(1)	78.87(7)
Ba(1)–O(13)	2.856(4)	Ba(1)–O(1)	2.910(2)	O(4)–Cu(1)–O(7)	153.5(2)	O(1)–Cu(1)–O(2)	76.14(9)
Cu(1)–O(4)	1.963(5)	Cu(1)–O(1)	1.957(2)	O(4)–Cu(1)–O(3)	75.03(19)	O(1)–Cu(1)–O(5)	155.11(9)
Cu(1)–O(7)	1.969(5)	Cu(1)–O(2)	1.980(2)	O(4)–Cu(1)–N(2)	97.7(2)	O(1)–Cu(1)–N(4)	97.38(11)
Cu(1)–O(3)	2.001(5)	Cu(1)–O(5)	1.993(2)	O(4)–Cu(1)–O(1)	102.1(2)	O(1)–Cu(1)–O(4)	101.04(9)
Cu(1)–N(2)	2.071(6)	Cu(1)–N(4)	2.035(3)	O(3)–Cu(2)–O(5)	154.74(19)	O(2)–Cu(2)–O(1)	75.78(9)
Cu(1)–O(1)	2.174(5)	Cu(1)–O(4)	2.180(2)	O(3)–Cu(2)–O(4)	75.16(19)	O(2)–Cu(2)–O(7)	150.02(9)
Cu(1)–Cu(2)	2.9348(11)	Cu(1)–Cu(2)	2.9053(5)	O(3)–Cu(2)–N(1)	96.3(2)	O(2)–Cu(2)–N(3)	97.47(10)
Cu(2)–O(3)	1.966(5)	Cu(2)–O(2)	1.965(2)	O(3)–Cu(2)–O(2)	101.49(19)	O(2)–Cu(2)–O(3)	105.82(9)
Cu(2)–O(5)	1.968(5)	Cu(2)–O(1)	1.988(2)	O(13)–Cu(3)–O(10)	153.90(19)	O(13)–Cu(3)–O(14)	75.56(9)
Cu(2)–O(4)	1.992(5)	Cu(2)–O(7)	1.988(2)	O(13)–Cu(3)–O(14)	75.94(18)	O(13)–Cu(3)–O(10)	151.28(9)
Cu(2)–N(1)	2.060(6)	Cu(2)–N(3)	2.020(3)	O(13)–Cu(3)–N(3)	96.4(2)	O(13)–Cu(3)–N(2)	97.39(10)
Cu(2)–O(2)	2.153(5)	Cu(2)–O(3)	2.202(2)	O(13)–Cu(3)–O(15)	104.28(19)	O(13)–Cu(3)–O(15)	103.58(9)
Cu(3)–O(13)	1.958(5)	Cu(3)–O(13)	1.970(2)	O(12)–Cu(4)–O(14)	152.98(18)	O(14)–Cu(4)–O(13)	75.48(9)
Cu(3)–O(10)	1.972(5)	Cu(3)–O(14)	1.982(2)	O(12)–Cu(4)–O(13)	93.75(19)	O(14)–Cu(4)–O(12)	151.04(9)
Cu(3)–O(14)	1.990(5)	Cu(3)–O(10)	2.013(2)	O(12)–Cu(4)–N(4)	90.1(2)	O(14)–Cu(4)–N(1)	97.54(10)
Cu(3)–N(3)	2.053(6)	Cu(3)–N(2)	2.021(3)	O(12)–Cu(4)–O(16)	106.30(19)	O(14)–Cu(4)–O(16)	105.60(9)
Cu(3)–O(15)	2.153(5)	Cu(3)–O(15)	2.188(2)				
Cu(3)–Cu(4)	2.9289(10)	Cu(3)–Cu(4)	2.8958(5)				
Cu(4)–O(12)	1.976(4)	Cu(4)–O(14)	1.965(2)				
Cu(4)–O(14)	1.980(4)	Cu(4)–O(13)	1.990(2)				
Cu(4)–O(13)	2.004(5)	Cu(4)–O(12)	2.002(2)				
Cu(4)–N(4)	2.052(6)	Cu(4)–N(1)	2.019(3)				
Cu(4)–O(16)	2.182(5)	Cu(4)–O(16)	2.177(2)				

two distinct sets of Ba–O bonds, the molecular structures of complexes **1** and **2** display sandwich-like features similar to those found in the $YBa_2Cu_3O_{7-x}$ structure. The geometry of the $BaCu_4$ units can be best described as two triangles sharing a corner.

All the metal centers are connected with each other due to the bridging nature of the ligands. The oxygen atoms of dmap ligands function as μ_3-bridges between each two copper and one barium atom. This type of bridging of three metal centers by the oxygen atom of an amino alcohol ligand has been observed previously.[28] Four out of the six acetate ligands are bridging between copper and barium atoms while the remaining two are bridging between the two copper centers in the dicopper units at the apex of the molecule.

Thermal decomposition of complexes 1 and 2

The thermal behavior of complexes **1** and **2** has been examined by thermogravimetric analysis, performed under an atmosphere of flowing nitrogen gas (25 ml min^{-1}) with heating rates of 10 °C min^{-1}. The TGA/DTA curve of complex **1** shows three stages of weight loss (Fig. 3a). The first step begins at 20 °C and is completed at 165 °C with a weight loss of 11.85%. The second step starts at 165 °C and is completed at 289 °C giving a maximum weight loss of 47.15%. The last weight loss starts at 289 °C and is completed at 412 °C resulting in a residue amounting to 31.10% of the initial weight. The residual weight (31.10%) is in good agreement with the expected composition for $BaCu_4O_5$ (31.82%). In contrast the TGA/DTA curve of complex **2** (Fig. 3b) shows

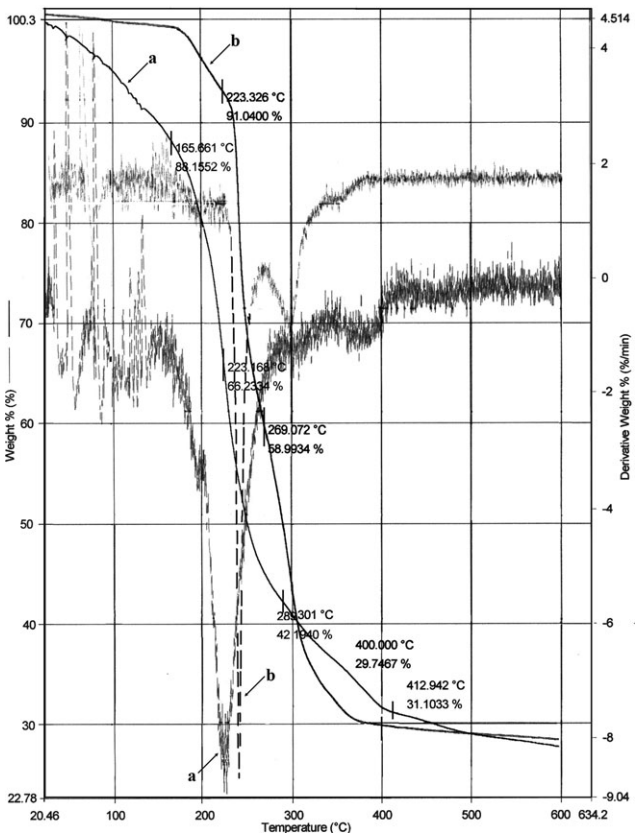

Fig. 3 Thermogravimetric plot showing loss in weight with increase in temperature (a) for complex **1** and (b) for complex **2**.

two stages of weight loss. The first step begins at 200 °C and is completed at 269 °C with a maximum weight loss of 42.10%. The second one starts at 269 °C and is completed at 400 °C, resulting in a residue amounting to 29.74% of the initial weight which is slightly less, but close to the expected composition for $BaCu_4O_5$ (32.06%), indicating that the complexes decompose quantitatively to composite oxides. The IR spectra of the TGA residues also prove the removal of carboneous matter from the organic groups leaving a final residue corresponding to composite oxides. In the complexes **1** and **2** each metal centre is coordinatively saturated by the oxygen atoms of the chelating carboxylate and dmap ligands thus eliminating the need for additional oxygen to form oxides. Thus the new robust precursors are suitable for deposition of clean barium copper oxide thin films at the relatively low temperatures of 400 and 450 °C.

The X-ray diffractograms of the thin films deposited from complexes **1** and **2** (Fig. 4) indicate the formation of composites of two different types of oxide phases.

The composite oxides exist as highly crystalline phases with mass ratios of 49 to 51% for $BaCuO_2$ and CuO, respectively, This corresponds to a mole ratio of 1 : 3 in favor of CuO, or an altogether formula $BaCu_4O_5$, which is in excellent agreement with the values obtained in the TGA experiment. CuO[29] found after both reactions is in the form of tenorite with the monoclinic space group $C2/c$ with cell parameters of a = 4.684 Å, b = 3.425 Å, c = 5.129 Å, and β = 99.47°, while the barium–copper oxide $BaCuO_2$[30] has a body centered cubic lattice system with the space group $Im\text{-}3m$. The XRD peak pattern also closely matches that of another barium–copper oxide $Ba_2Cu_3O_{5-x}$[31] with the assigned tetragonal space group $P4_2/mcm$, but on the basis of peak intensities and 2θ values the matching with $BaCuO_2$ is more likely than $Ba_2Cu_3O_{5-x}$. In the XRD patterns the peaks at 39.10° correspond to both $BaCuO_2$ and CuO. The peaks corresponding to CuO are marked in Fig. 4 while all other peaks correspond to $BaCuO_2$. There is no evidence of fluorine contamination in sample (b). IR spectra of the TGA residues do not show any C–O stretching vibration bands, indicative of the absence of carbonates. For complex **2** the presence of the fluorinated ligands might have played a role in inhibiting the formation

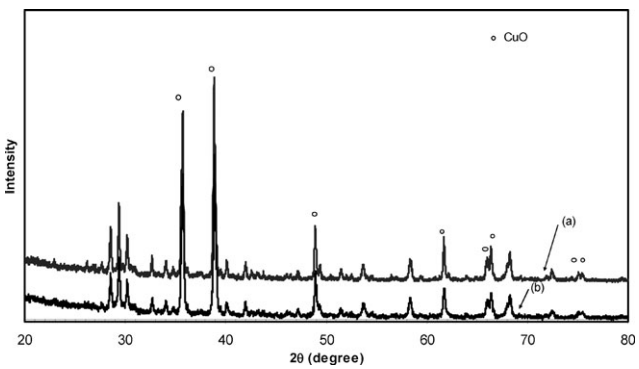

Fig. 4 X-Ray diffractograms of oxides obtained from (a) complex **1** and (b) complex **2**. ∘ indicates the peaks originated from CuO, all other peaks are related to the $BaCuO_2$ phase.

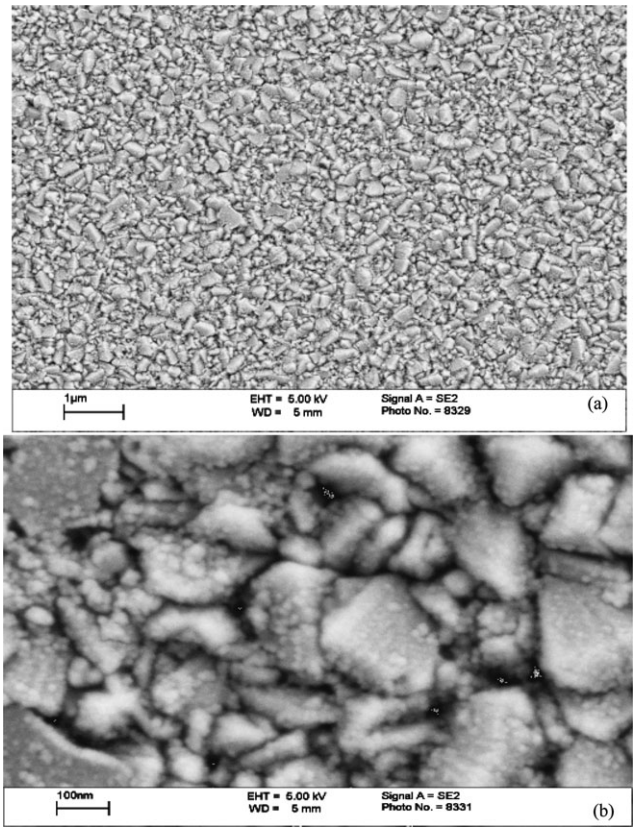

Fig. 5 SEM images of thin films deposited from complex **1** at 450 °C (a) at low and (b) at high resolution.

of $BaCO_3$.[32] It has been reported that fluorine containing precursors in the formation of superconductor thin films have the advantage of inhibiting the formation of $BaCO_3$ by intermediate formation of BaF_2, which is easier to decompose than $BaCO_3$ without deteriorating the quality of the YBCO during firing.[33,34]

The films exhibit a good adhesion to the substrate as verified by the "Scotch Tape" test and are stable towards air and moisture. Scanning electron microscopic (SEM) images (Fig. 5 and Fig. 6) of an oxide thin film deposited from complexes **1** and **2** show smooth and compact film morphologies with homogenously dispersed particles. The mean average particle sizes are 105–175 nm and 110–205 nm for material obtained from complex **1** and **2**, respectively, and the grains are well defined with clear boundaries. The high resolution SEM micrographs (Fig. 5b and Fig. 6b) also show that the film deposited from complex **2** is denser and more uniform than that from complex **1**. An energy dispersive X-ray analysis of the thin films deposited from precursors **1** and **2** indicates that the metallic ratio of Ba : Cu in both the complexes is 1 : 4 which also supports the even distribution of both the phases.

Conclusions

The present work is focused on the easy preparation of single source heterobimetallic complexes, having a high solubility and stability, which decompose to homogeneously dispersed

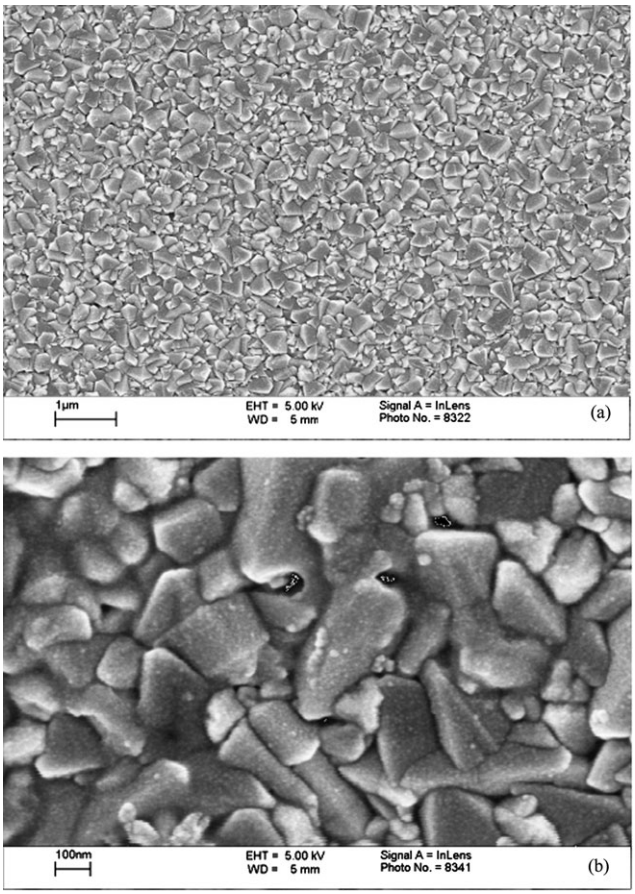

Fig. 6 SEM images of thin films deposited from complex **2** at 400 °C (a) at low and (b) at high resolution.

composite metal oxides. The heterobimetallic complexes **1** and **2** were synthesized by simple and routine chemical reactions of $Ba(dmap)_2$ with $Cu(OAc)_2$ for **1** and $Cu(TFA)_2$ for **2**, under ordinary reaction conditions. Thermal decomposition studies show that the general idea of combining a copper precursor moiety with barium moieties in a single molecule results in a copper barium oxide composite ($BaCuO_2$–CuO), in a single step. Further studies of this and related systems can now open new approaches to the synthesis of thin films and nanoparticles of potential superconductors for advanced technological and industrial applications.

Acknowledgements

AAT and MM acknowledge the Pakistan Science Foundation for funding through Project No. PSF/RES/C-QU/CHEM.(408). The Smart Apex diffractometer was funded by NSF grant 0087210, by Ohio Board of Regents grant CAP-491, and by YSU.

References

1 M. W. Rupich, B. Lagos and J. P. Hachey, *Appl. Phys. Lett.*, 1989, **55**, 2447.
2 D. Segal, *Chemical Synthesis of Advanced Ceramic Material*, Cambridge University Press, Cambridge, 1989.
3 D. C. Bradley, *Chem. Rev.*, 1989, **89**, 1317.
4 J. Zhao, K. Dahmen, H. Marcy, T. J. Marks, B. W. Wessels and C. R. Kannewurf, *Appl. Phys. Lett.*, 1988, **53**, 1750.
5 *High Tc Superconductor Thin Films*, ed. L. Correra, Elsevier Science Publishers, Amsterdam, 1992.
6 F. A. Cotton and G. Wilkinson, *Advanced Inorganic Chemistry*, John Wiley & Sons, New York, 5th edn, 1988, pp. 11.
7 M. Hamid, A. A. Tahir, M. Mazhar, F. Ahmad, K. C. Molloy and G. Kociok-Kohn, *Inorg. Chim. Acta*, 2008, **361**, 188.
8 M. Hamid, A. A. Tahir, M. Mahzar, M. Zeller and A. D. Hunter, *Inorg. Chem.*, 2006, **45**, 10457.
9 J. Ribas, M. Monfort, R. Costa and X. Solans, *Inorg. Chem.*, 1993, **32**, 695.
10 M. S. El Fallah, E. Rentschler, A. Caneschi, R. Sessoli and D. Gatteschi, *Inorg. Chem.*, 1996, **35**, 3723.
11 *Bruker Advanced X-Ray Solution SMART for WNT/2000 (Version 5.628)*, Bruker AXS Inc., Madison, Wisconsin, USA, 1997–2003.
12 *Bruker Advanced X-Ray Solution SAINT (Version 6.45)*, Bruker AXS Inc., Madison, Wisconsin, USA, 1997–2003.
13 *Bruker Advanced X-Ray Solution SHELXTL (Version 6.14)*, Bruker AXS Inc., Madison, Wisconsin, USA, 2003.
14 A. A. Tahir, K. C. Molloy, M. Mazhar, G. Kociok-Köhn, M. Hamid and S. Dastgir, *Inorg. Chem.*, 2005, **44**, 9207.
15 D. C. Bradley, R. C. Mehrotra and D. P. Gaur, *Metal Alkoxides*, Academic Press, London, 1987.
16 A. A. Tahir, M. Hamid, M. Mazhar, M. Zeller, A. D. Hunter, M. Nadeem and M. J. Akhtar, *Dalton Trans.*, 2008, 1224.
17 M. Hamid, A. A. Tahir, M. Mahzar, M. Zeller and A. D. Hunter, *Inorg. Chem.*, 2007, **46**, 4120.
18 S. Wang, *Polyhedron*, 1998, **17**, 831.
19 D. H. Gibson, Y. Ding, R. L. Miller, B. A. Slead, M. S. Mashuta and J. F. Richardson, *Polyhedron*, 1999, **18**, 1189.
20 J. Zhang, L. G. Hubert-Pfalzgraf and D. Luneau, *Polyhedron*, 2005, **24**, 1185.
21 J. C. Zheng, R. J. Rousseau and S. Wang, *Inorg. Chem.*, 1992, **31**, 106.
22 S. Wang, S. J. Trepanier, J. C. Zheng, Z. Pang and M. J. Wagner, *Inorg. Chem.*, 1992, **31**, 2118.
23 M. Melnik, *Coord. Chem. Rev.*, 1982, **42**, 259.
24 S. Wang, S. J. Trepanier and M. Wagner, *Huaxue Xuebao*, 1993, **32**, 833.
25 K. G. Caulton, M. H. Chisholm, S. R. Drake and K. Folting, *Inorg. Chem.*, 1991, **30**, 1500.
26 C. P. Love, C. C. Torardi and C. J. Page, *Inorg. Chem.*, 1992, **31**, 1784.
27 M. F. Garbauskas, R. H. Arendt and J. S. Kaspar, *Inorg. Chem.*, 1987, **26**, 3191.
28 M. Hamid, A. A. Tahir, M. Mahzar, K. C. Molloy and G. Kociok-Köhn, *Inorg. Chem. Commun.*, 2008, **11**, 1160.
29 (*a*) ICDD powder diffraction database file card number [00-005-0661]; (*b*) H. E. Swanson and E. Tatge, *Natl. Bur. Stand. Circ. (U. S.)*, 1953, **539**, 49.
30 ICDD powder diffraction database file card number [00-038-1402].
31 (*a*) ICDD powder diffraction database file card number [00-040-0312]; (*b*) I. Halasz, V. Fulop, I. Kirschner and T. Porjesz, *J. Cryst. Growth*, 1988, **91**, 444.
32 T. Araki and I. Hirabayashi, *Supercond. Sci. Technol.*, 2003, **16**, R71.
33 T. Kumagai, T. Manabe, W. Kondo, H. Minamiue and S. Mizuta, *Jpn. J. Appl. Phys.*, 1990, **29**, L940.
34 F. Parmigiani, G. Chiarello, N. Ripamonti, H. Foretzki and U. Roll, *Phys. Rev. B: Condens. Matter Mater. Phys.*, 1987, **36**, 7148.